Evolution of Fermi surface and normal-state gap in the chemically substituted cuprates $Bi_2Sr_{2-x}Bi_xCuO_{6+\delta}$

Z.-H. Pan,[1] P. Richard,[1] Y.-M. Xu,[1] M. Neupane,[1] P. Bishay,[1] A. V. Fedorov,[2] H. Luo,[3] L. Fang,[3] H.-H. Wen,[3] Z. Wang,[1] and H. Ding[1,*]

[1]*Department of Physics, Boston College, Chestnut Hill, Massachusetts 02467, USA*

[2]*Advanced Light Source, Lawrence Berkeley National Laboratory, Berkeley, California 94720, USA*

[3]*National Laboratory for Superconductivity, Institute of Physics, and National Laboratory for Condensed Matter Physics, P.O. Box 603, Beijing 100080, People's Republic of China*

(Received 22 September 2008; revised manuscript received 29 December 2008; published 31 March 2009)

We have performed a systematic angle-resolved photoemission study of chemically substituted cuprates $Bi_2Sr_{2-x}Bi_xCuO_{6+\delta}$. We observed that the Fermi-surface area shrinks linearly with Bi-substitution content x, reflecting the electron doping nature of this chemical substitution. In addition, the spectral linewidth broadens rapidly with increasing x and becomes completely incoherent at the superconducting-insulating boundary. The d-wave-like normal-state gap observed in the lightly underdoped region gradually evolves into a large soft gap, which suppresses antinodal spectral weight linearly in both the excitation energy and temperature. Combining with the bulk resistivity data obtained on the same samples, we establish the emergence of the Coulomb gap behavior in the very underdoped regime. Our results reveal the dual roles, doping and disorder, of off-plane chemical substitutions in high-T_c cuprates and elucidate the nature of the quantum electronic states due to strong correlation and disorder.

DOI: 10.1103/PhysRevB.79.092507 PACS number(s): 74.72.Hs, 74.25.Fy, 79.60.−i

Since high-temperature superconductivity in cuprates is achieved by adding extra carriers into an antiferromagnetic Mott insulator, how the electronic structures, such as Fermi surface (FS) and energy gap (including the superconducting gap and the normal-state pseudogap), evolve with doping is critical to understanding the elusive superconducting mechanism. Direct spectroscopic probe of the electronic structures, such as angle-resolved photoemission spectroscopy (ARPES) and scanning tunneling microscopy (STM), are mostly done on the $Bi_2Sr_2Ca_nCu_{n+1}O_{2n+6}$ compounds, whose doping range is limited through oxygenation. More heavily underdoping can only be achieved by chemical substitution.[1,2] By substituting trivalent Bi ions for divalent Sr ions into the apical plane of $Bi_2Sr_2CuO_{6+\delta}$ (Bi2201), we have further pushed the underdoping threshold continuously to the insulating phase.[3] We establish a concrete linear relationship between the reduction in the hole concentration and the Bi substitution through ARPES by measuring the reduction in the Luttinger volume enclosed by the FS. In addition, we observe that quasiparticle (QP) coherence vanishes at the superconducting-insulating boundary. More importantly, the d-wave-like pseudogap observed in the lightly underdoped region gradually evolves into a large soft gap, which suppresses antinodal spectral weight linearly in both the excitation energy and temperature. We propose that the pseudogap in the underdoped regime evolves into a Coulomb gap (CG) beyond the superconducting-insulating phase boundary. To support this finding, we performed transport measurements on the same samples and found that the resistivity data are consistent with hopping transport in the presence of a Coulomb gap in the highly underdoped regime, characteristic of strongly disordered correlated systems. The Coulomb energy scale derived from transport agrees remarkably well with the gap energy in the ARPES spectra. The observed universality of this pseudogap evolution reveals the dual roles, underdoping and disorder, of chemical substitution in high-T_c cuprates.

High-quality single crystals of $Bi_2Sr_{2-x}Bi_xCuO_{6+\delta}$ (Bi-Bi2201) were grown by the traveling solvent floating zone method. T_c of superconducting samples were determined by ac susceptibility; the superconducting transition width is about 0.5–1.3 K. More technical details have been described previously.[3] ARPES experiments were performed at the beamline U1NIM of the Synchrotron Radiation Center in Wisconsin and the beamline 12.0.1 of the Advanced Light Source in California. Energy and momentum resolutions have been set to ~10–20 meV and ~0.02 Å^{-1}, respectively. All samples were cleaved and measured *in situ* in a vacuum better than 8×10^{-11} Torr on a flat (001) surface.

We show in Fig. 1 the evolution of the Fermi surface of $Bi_2Sr_{2-x}Bi_xCuO_{6+\delta}$ at 20 K for six different Bi contents from $x=0.05$ to 0.4. The Fermi vectors extracted from the momentum distribution curve (MDC) peaks are consistent with the intensity plots and allow a precise determination of the underlying FS, which is defined as a contour of the minimum gap locus.[4] We report in Fig. 1(g) all the underlying FS extracted for the various Bi concentrations using an effective tight-binding fit. We notice a smooth evolution in the shape of the FS. In particular, the FS at the antinodes moves away from the $M(\pi,0)$ point as the Bi content increases. More importantly, as shown more clearly in Fig. 1(g), the size of the $Y(\pi,\pi)$-centered holelike FS decreases continuously with the Bi concentration, indicating the underdoping nature of the $Sr^{2+}\rightarrow Bi^{3+}$ substitution.

We extract experimental values of the effective hole doping p and plot them as a function of the Bi substitution x in Fig. 1(h) by using Luttinger theorem, which states that the volume of an enclosed FS is proportional to the carrier concentration $1+p$. While the derived doping p decreases linearly with x, as shown in Fig. 1(h), the linear fit gives p

 ©2009 The American Physical Society

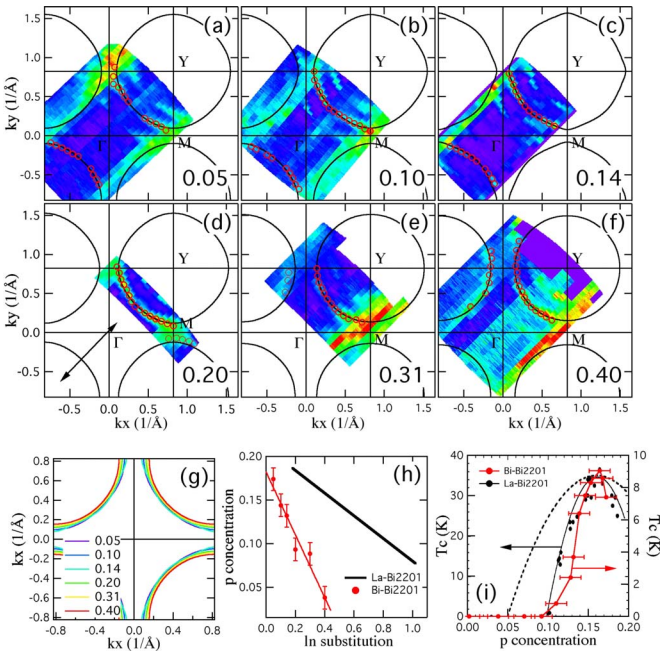

FIG. 1. (Color online) FS mapping of $Bi_2Sr_{2-x}Bi_xCuO_{6+\delta}$ at different Bi contents. [(a)–(f)] Plots of ARPES intensity integrated within $\omega=0\pm12$ meV for $x=0.05$, 0.1, 0.14, 0.2, 0.31, and 0.4. The red circles are extracted from MDC peaks, and the lines are the tight-binding fits to the circles. All the samples are aligned along ΓY parallel to A, as shown by the arrow in (d). (g) FS contours from the tight-binding fits. (h) Doping effect induced by the substitution of Bi (dots) (the thin line is the best linear fit) and La (solid line) measured by Hall measurements (Ref. 5). (i) Corresponding phase diagrams of Bi-Bi2201 and La-Bi2201 in comparison to a generic phase diagram of the high-T_c cuprates (Ref. 7).

$=0.182-0.36x$, which indicates that each substituting Bi atom removes only 0.36 holelike carrier from the CuO_2 plane. A similar result, albeit with an even smaller doping efficiency, has been observed in $Bi_2Sr_{2-x}La_xCuO_{6+\delta}$ (La-Bi2201) by Hall measurements,[5] also plotted in Fig. 1(h) as a comparison. The reason for this surprising behavior is not clear yet. Although one would expect that instead of the usual trivalent ions, the divalent ions of Bi or La could be present, measurements of Bi core levels in our samples are inconsistent with this hypothesis. One possibility to explain this phenomenon is that the oxygen dopant concentration δ, which is not known precisely in these materials, increases with x, compensating the extra charge of the Bi^{3+} ion and maintaining a total charge neutrality $2\delta=p+x$. Spectroscopic evidence has led to a similar scenario for the electron-doped cuprates, where the Ce^{4+} dopant ions tend to form pairs with the extraneous oxygen ions.[6]

In Fig. 1(i), we construct the phase diagram of Bi-Bi2201 based on transport/susceptibility measurements[3] and the relationship of p vs x displayed in Fig. 1(h). This phase diagram, when rescaled along the temperature axis, matches well with the one constructed from the Hall measurements of the La-Bi2201.[5] We note that in both Bi- and La-substituted samples, T_c vanishes around 10% hole concentration, which is larger than the 5% critical value found in many cuprates.[7] This suggests that underdoping is not the only effect introduced by the $Sr^{2+}\rightarrow Bi^{3+}$ substitution. Beyond the chemical doping necessary to vary the carrier concentration in cuprates, a host of experiments have provided evidences that the ionic and electronic structures outside the CuO_2 planes have important effects on the low-energy electronic states and the superconducting properties.[8–11] In particular, the substitution of Sr^{2+} by Ln^{3+} (Ln=La, La, Pr, Nd, Sm, Eu, Gd, and Bi) in $Bi_2Sr_{2-x}Ln_xCuO_{6+\delta}$ leads to a critical temperature that significantly depends on ion radius mismatch (Δr); at $x=0.4$, $T_c\sim30$ K for La substitution which has the smallest Δr while $T_c\sim0$ K for Bi substitution which has the largest Δr.[9] These results have been cited as evidence of strong dependence of T_c to apical site (A-site) disorder. However, our results suggest that this is not the complete story. As shown in Fig. 1(h), at the fixed substitution level $x=0.4$, the hole-doping levels are different for La-Bi2201 ($p\sim0.16$, optimally doped) and Bi-Bi2201 ($p\sim0.05$, heavily underdoped). Nevertheless, there is a factor of 3 in terms of the maximum T_c's in these two systems, suggesting the superconducting properties of $Bi_2Sr_{2-x}Ln_xCuO_{6+\delta}$ are influenced by both charge underdoping and lattice disorder, the dual characters associated with chemical substitution.

Another interesting phenomenon we observed is the dependence of the QP spectral coherence on the Bi content. In Fig. 2, we compare the near-nodal and antinodal energy distribution curve (EDC) line shapes for various Bi contents. Sharp EDC peaks are observed in both directions at low Bi-substitution levels. The peak broadens as x increases and is not observed in the heavily substituted samples. This loss of coherence is also accompanied by an opening of a soft energy gap characterized by the suppression of spectral weight in the vicinity of the Fermi energy (E_F). The crossover between the two regimes occurs around $x=0.20$, which corresponds to a doping of $p\sim0.1$, the superconducting-nonsuperconducting phase boundary at zero temperature. We plot the width of EDCs at k_F for the antinodal region in the inset of Fig. 2(b). One clearly sees a significant linewidth broadening when $p<0.1$, corresponding to $x>0.2$. This may suggest that the superconductivity is closely correlated with the QP coherence. We also note that the opening of this soft gap first appears in the antinodal region and spreads out to the nodal one upon increasing substitution, as indicated in Fig. 2. A similar but smaller nodal gap has been also observed previously in several lightly doped high-T_c cuprates and was attributed to disorder effect.[12]

Perhaps the most surprising finding from our study is the observation of different antinodal pseudogap behaviors at low and high Bi contents. The temperature dependence of the symmetrized antinodal EDCs is given in Figs. 3(a) and 3(b) for $x=0.2$ and $x=0.4$ samples, respectively. The antinodal gap is filled in and disappears above 80 K for the $x=0.2$ sample, similar to the conventional behavior of the pseudogap observed by STM for similar samples.[13] The larger gap of the $x=0.4$ sample behaves differently in the following ways: (1) it lacks a well-defined spectral structure to define the value of gap, although the suppression of spectral intensity starts from ~0.2 eV; (2) while its overall spectral shape is little affected within the temperature range up to 280 K, the intensity at E_F is linearly proportional to temperature, as shown in Fig. 3(d); (3) the spectral intensity is sup-

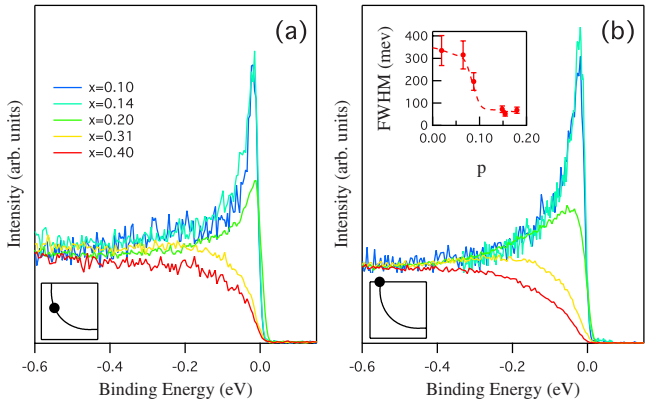

FIG. 2. (Color online) Comparison of EDC line shape of Bi-Bi2201 at different Bi contents. (a) Near the node and (b) near the antinode. The inset in (a) and (b) with black color show the k positions where those EDCs are taken. The inset in red color in (b) shows the full width at half maximum (FWHM) of antinodal EDCs at K_F. The dashed line is a guide to eyes.

pressed almost linearly in energy at low temperature, as shown in Fig. 3(c). The small nonzero intensity at E_F that makes the EDC look rounded could be due to the finite temperature and finite resolution. This reminds us of the classical CG (Ref. 14) or the granular behavior[15] in strongly disordered two-dimensional systems and suggest that the pseudogap in the underdoped regime has evolved into a Coulomb gap following the superconductor-insulator transition.

To test this finding, we performed transport measurements on the same samples to look for evidence of the Coulomb gap. The temperature dependence of the in-plane resistivity of $Bi_2Sr_{2-x}Bi_xCuO_{6+\delta}$ at different Bi content, x is plotted in Fig. 4 as the natural logarithm of resistivity versus $T^{-(1/2)}$. The superconductor-insulator transition around $x=0.2$ is clearly visible. For $x>0.2$, the resistivity curves show approximately linear behavior over a wider range of temperature, consistent with the classical hopping resistivity in the

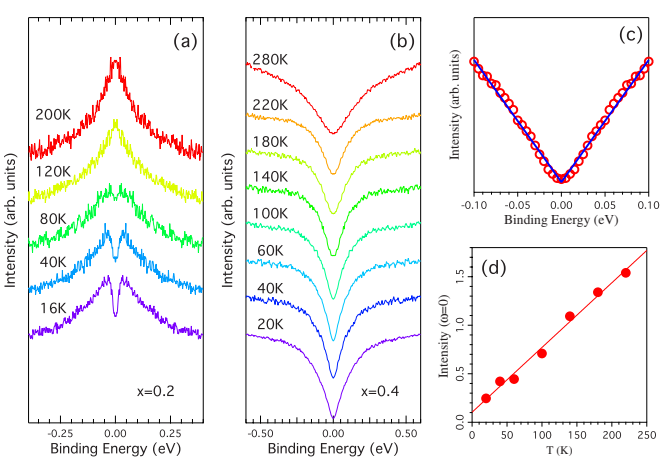

FIG. 3. (Color online) (a) Temperature dependence of symmetrized EDCs at K_F in the antinodal region for the $x=0.2$ sample and (b) for the $x=0.4$ sample. (c) Zoom-in view of the 20 K EDC shown in (b) near E_F and a linear fit to it. (d) Temperature dependence of EDC intensity at E_F (dots) and the corresponding linear fit (line) for the $x=0.4$ sample.

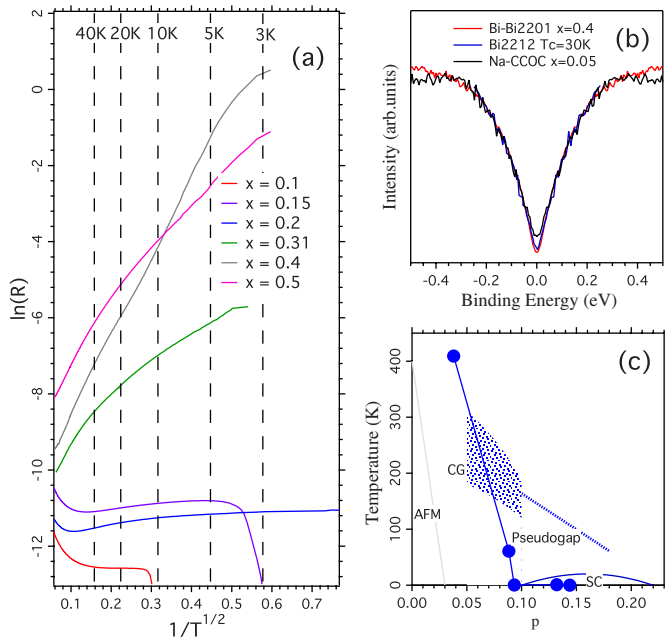

FIG. 4. (Color online) (a) Natural logarithm of resistivity versus $T^{-(1/2)}$ for samples $x=0.1$, 0.15, 0.2, 0.31, 0.4, and 0.5. (b) Line shape comparison of the antinodal EDCs in $Bi_2Sr_{1.6}Bi_{0.4}CuO_{6+\delta}$, $Bi_{2.1}Sr_2Ca_{1-x}Y_xCu_2O_8$ (from Ref. 16), and $Ca_{1.95}Na_{0.05}CuO_2Cl_2$ (from Ref. 17). (c) Qualitative phase diagram of $Bi_2Sr_{2-x}Bi_xCuO_{6+\delta}$.

presence of a Coulomb gap, $\rho(T)=\rho_0 \exp(T_0/T)^{1/2}$, expected for a disordered insulating system with long-range Coulomb interaction.[14] Here $T_0=e^2/\kappa\xi$ is the long-range Coulomb energy scale determined by the dielectric constant κ and the localization length ξ. From the slope of T-dependent curves in Fig. 4(a), we obtain T_0 and plot them in Fig. 4(c) (blue dots). For the $x=0.4$ sample, $T_0\sim 400$ K, which explains qualitatively the soft gap in the antinodal spectrum visible even at $T=280$ K shown in Fig. 3(b). Indeed, extrapolating the linear T dependence of ARPES intensity at E_F [shown in Fig. 3(d)] allows a rough estimate of the crossover temperature $T^*_{CG}\sim 500$ K, above which the suppression of the spectral weight ("gap") is completely filled. Thus the crossover temperature (T^*_{CG}) obtained from ARPES is consistent with T_0 derived from the resistivity, suggesting that the same Coulomb energy scale is involved in both ARPES and transport.

The ARPES spectra shown in Fig. 3(b) allow an estimate of the magnitude of the energy gap at the antinode for the $x=0.4$ sample, $\Delta\sim 0.19$ eV. This, combined with the derived value of $T_0\sim 400$ K for the same sample [see Fig. 4(c)], gives a ratio of $\Delta/T_0\sim 5$. It is known from the theory of the classical Coulomb gap,[14] $\Delta/T_0=g_0(\xi)^2T_0$ where g_0 is unperturbed density of states (DOS). A reasonable value of $g_0\sim 2.1$ state/eV cell was provided by band theory for Bi2201.[18] Taking $\xi\sim 8$ unit cells, we estimate that the ratio predicted by the Coulomb gap theory to be ~ 5. This remarkable qualitative agreement between the experimental ratio and theoretical one strongly supports the Coulomb gap nature of the observed soft gap in the photoemission spectra. It is interesting to note that T_0 becomes smaller as the Bi content decreases and becomes zero as x becomes 0.2, the

superconductor-insulator boundary revealed by the combined effects of underdoping and disorder. We caution here that the conventional Coulomb gap usually referred to the linear suppression of the DOS in an isotropic system and not to the spectral function measured near the antinodal region of a highly anisotropic material. Nevertheless, the antinodal intensity dominates the DOS in the hole-doped cuprates due to the Van Hove singularity.

A natural question to ask is how universal this Coulomb gap behavior is in the heavily underdoped high-T_c cuprates achieved by chemical substitution. To answer this question, we compared the antinodal EDC of the $x=0.4$ sample with heavily underdoped $Bi_{2.1}Sr_2Ca_{1-x}Y_xCu_2O_8$ ($T_c \sim 30$ K) (Ref. 16) and nonsuperconducting $Ca_{1.95}Na_{0.05}CuO_2Cl_2$ (Na-CCOC),[17] as shown in Fig. 4(b). We found that the line shape of these different samples are very similar, characterized by the opening of a large soft gap and the absence of the QP peak.

Interestingly, as shown in the case of $Bi_{2.1}Sr_2Ca_{1-x}Y_xCu_2O_8$,[16] the antinodal leading-edge gap was found to increase upon more underdoping, while the near-nodal gap seems to decrease and be proportional to T_c. This apparent gap dichotomy (or two-gap scenario) has been interpreted as evidence that the *d*-wave pairing gap opens along the FS arc around the node while the antinodal gap is a different type of gap that may not contribute to superconductivity.[16] However, with the appearance of a Coulomb gap in heavily substituted/underdoped samples, we raise another possibility, as summarized in the schematic phase diagram shown in Fig. 4(c); upon increasing underdoping, the *d*-wave-like leading-edge gap region may be influenced or even truncated by the Coulomb gap region, which by itself is induced by the intrinsic disorder associated with chemical substitution. While this Coulomb gap region might push the onset of the superconducting phase to a higher doping level, as observed in the substituted Bi2201, it may also result in a spin-glass phase often observed between the antiferromagnetic insulating phase and the superconducting state at low temperatures.

This work was supported by grants from the U.S. NSF under Contracts No. DMR-0353108 and No. DMR-0704545 and the DOE under Contract No. DEFG02-99ER45747. This work was based on the research conducted at the Synchrotron Radiation Center supported by NSF under Contract No. DMR-0537588 and the Advanced Light Source supported by DOE under Contract No. DE-AC02-05CH11231. The work at the IOP, Beijing was supported by the NSFC, the MOST 973 project (Contracts No. 2006CB601000 and No. 2006CB921802), and the CAS project ITSNEM.

*dingh@bc.edu

[1] K. Tanaka *et al.*, Phys. Rev. B **70**, 092503 (2004).
[2] A. Kanigel *et al.*, Nat. Phys. **2**, 447 (2006).
[3] H. Luo *et al.*, J. Cryst. Growth **305**, 222 (2007).
[4] H. Ding, M. R. Norman, T. Yokoya, T. Takeuchi, M. Randeria, J. C. Campuzano, T. Takahashi, T. Mochiku, and K. Kadowaki, Phys. Rev. Lett. **78**, 2628 (1997).
[5] Y. Ando, Y. Hanaki, S. Ono, T. Murayama, K. Segawa, N. Miyamoto, and S. Komiya, Phys. Rev. B **61**, R14956 (2000).
[6] G. Riou, P. Richard, S. Jandl, M. Poirier, P. Fournier, V. Nekvasil, S. N. Barilo, and L. A. Kurnevich, Phys. Rev. B **69**, 024511 (2004).
[7] M. R. Presland *et al.*, Physica C **176**, 95 (1991).
[8] J. P. Attfield, A. L. Kharlanov, and J. A. McAllister, Nature (London) **394**, 157 (1998).
[9] H. Eisaki, N. Kaneko, D. L. Feng, A. Damascelli, P. K. Mang, K. M. Shen, Z. X. Shen, and M. Greven, Phys. Rev. B **69**, 064512 (2004).
[10] K. McElroy *et al.*, Science **309**, 1048 (2005).
[11] P. Richard, Z. H. Pan, M. Neupane, A. V. Fedorov, T. Valla, P. D. Johnson, G. D. Gu, W. Ku, Z. Wang, and H. Ding, Phys. Rev. B **74**, 094512 (2006).
[12] K. M. Shen *et al.*, Phys. Rev. B **69**, 054503 (2004).
[13] M. Kugler, O. Fischer, C. Renner, S. Ono, and Y. Ando, Phys. Rev. Lett. **86**, 4911 (2001).
[14] A. L. Efros and B. I. Shklovskii, J. Phys. C **8**, L49 (1975).
[15] I. S. Beloborodov, K. B. Efetov, A. V. Lopatin, and V. M. Vinokur, Phys. Rev. Lett. **91**, 246801 (2003).
[16] K. Tanaka *et al.*, Science **314**, 1910 (2006).
[17] K. Shen *et al.*, Science **307**, 901 (2005).
[18] M. S. Hybertsen and L. F. Mattheiss, Phys. Rev. Lett. **60**, 1661 (1988).